

# Parton saturation at strong coupling from AdS/CFT

Edmond Iancu

*Institut de Physique Théorique de Saclay, F-91191 Gif-sur-Yvette, France*

---

## Abstract

I describe the parton picture at strong coupling emerging from the gauge/gravity duality, with emphasis on the universality of the phenomenon of parton saturation. I discuss several consequences of this picture for the phenomenology of a strongly coupled quark–gluon plasma, which are potentially relevant for heavy ion collisions at RHIC and LHC.

---

## 1. Introduction: Why study saturation at strong coupling ?

Since the idea of parton saturation has first emerged [1, 2], in the mid eighties, as a possible solution to the unitarity problem in QCD at high energy, this phenomenon has been generally associated with weak coupling. This was based on the asymptotic freedom of QCD together with the following, self-consistent, argument: in the kinematical domain for saturation, one expects parton densities to be large, hence the relevant values of the QCD running coupling should be weak; and indeed calculations in QCD at weak coupling ( $\alpha_s \ll 1$ ) predict large gluon occupation numbers at saturation,  $n \sim 1/\alpha_s \gg 1$ , thus closing the argument. Following this logic, and also by lack of non-perturbative tools, all the subsequent studies of this phenomenon from first principles were performed within perturbative QCD, with increasingly higher degrees of sophistication [3] (and Refs. therein). In particular, the observation that a regime characterized by high occupation numbers and weak coupling is semi-classical [4] paved the way to the modern effective theory for gluon saturation within pQCD, which is the Color Glass Condensate (CGC) [3]. These studies demonstrated the existence of an intrinsic scale associated with this phenomenon, the *saturation momentum*  $Q_s$  — the transverse momentum below which non-linear effects in the gluon distribution become important —, which increases quite fast with the energy, and thus eventually becomes ‘hard’ ( $Q_s \gg \Lambda_{\text{QCD}} \simeq 200$  MeV). This scale also controls the gluon density at and near saturation, and hence it sets the scale for the running coupling in the approach towards saturation. All these results have confirmed the original intuition that, *for sufficiently high energies*, parton saturation is a weak coupling phenomenon which is driven by the rapid evolution of the gluon distribution via bremsstrahlung.

But what about the *current* energies, as attained in the present days colliders ? These energies are relatively high, allowing to explore values of the Bjorken’s  $x$  variable —

---

*Email addresses:* Edmond.Iancu@cea.fr (Edmond Iancu)

the longitudinal momentum fraction of a parton inside the hadron wavefunction — as small as  $x \sim 10^{-4}$  at RHIC,  $10^{-5}$  at HERA and even  $10^{-6}$  at the LHC. Besides, in collisions involving large nuclei, the gluon density and thus the saturation momentum are further enhanced by the atomic number  $A \gg 1$ . Yet, in spite of such favorable circumstances, the corresponding values of  $Q_s$  remain quite modest: this scale does not exceed 1.5 GeV at HERA and RHIC (with nuclei) and it should be around  $2 \div 3$  GeV in the ‘forward’ kinematics at the LHC. Moreover, the theoretical analyses of the phenomenology initiate the high-energy evolution at some intermediate value  $x_0$  which must be small enough to justify the focus on the evolution with increasing energy (as opposed, e.g., to the DGLAP evolution), but large enough (with respect to the  $x$  values of interest) to minimize the effects of the uncertainties in the initial conditions at  $x_0$  (which must be taken from a model, so like the McLerran–Venugopalan model [4]). This value  $x_0$  and the associated saturation momentum  $Q_s(x_0)$  are generally chosen in such a way to optimize the description of some set of data, so like the HERA data for the DIS structure function  $F_2$ , and some typical values (taken from Ref. [5]) are  $x_0 \sim 0.01$  and  $Q_s^2(x_0) \sim 0.4 \text{ GeV}^2$ . For such ‘semihard’ values  $Q_s$ , the weak coupling techniques are only marginally applicable.

So, clearly, it would be very interesting to have some (at least, qualitative) understanding of the phenomenon of parton saturation in the transition region towards strong coupling. In general, that problem is extremely complicated not only because the coupling is strong, but especially because of the possible mixing with the physics of confinement, for which there is no analytic understanding from first principles. It is therefore both interesting and remarkable that there exists a physical regime of QCD, in which one can isolate the physics of (relatively) strong coupling from that of confinement, and which moreover might have some relevance for the present day phenomenology, as suggested by some of the data at RHIC. This refers to the deconfined phase of QCD, the *quark–gluon plasma* (QGP), which in thermodynamical equilibrium exists for temperatures larger than a critical value  $T_c \simeq 170 \text{ MeV}$ . This phase has been rather extensively studied (at least, in so far as its thermodynamical properties are concerned) via lattice QCD calculations. By now we have rather firm evidence that it has been also experimentally produced at RHIC, in the intermediate stages of the heavy ion collisions [6]. There are moreover strong indications that the partonic matter liberated by the collision equilibrates quite fast, over a time  $\tau_0 \sim 1 \text{ fm}/c$ , at a temperature  $T = (2 \div 3)T_c$ , and then lives in the plasma phase for about  $5 \text{ fm}/c$ , before eventually cooling down and hadronizing. (In lead–lead collisions at LHC, one should reach  $T \sim 5T_c$  and a QGP lifetime  $\tau \sim 10 \text{ fm}/c$ .)

In the forthcoming two sections, I shall argue that: (i) there are strong indications, notably from the heavy ion experiments at RHIC, that this deconfined matter is effectively strongly coupled, (ii) the physics of parton saturation in a strongly coupled plasma is interesting not only at a conceptual level, but also for the phenomenology at RHIC, and (iii) this physics can be reliably studied, at least at a qualitative level, by using the gauge/gravity duality. Then, in the remaining part of the discussion, I will explain the consequences of this approach for parton evolution and saturation at strong coupling.

## 2. sQGP at RHIC

There are several arguments why the quark–gluon plasma produced at RHIC or LHC can be considered as strongly coupled. At a formal level, one can note that the relevant temperatures are relatively low (less than 1 GeV), so the respective QCD coupling is quite high:  $\alpha_s \equiv g^2/4\pi \simeq 0.4$ , or  $g \simeq 2$ . Moreover, unlike at zero temperature, where the perturbative expansion is a series in powers of  $\alpha_s$ , at finite temperature this is truly a series in powers of  $g$  and it shows very bad convergency unless  $g \ll 1$  (which in QCD requires astronomically high temperatures) [7]. But this formal argument is not decisive by itself, as shown by the following fact: one has demonstrated that appropriate resummations of the perturbative expansion are able to cure the problem of the lack of convergency and thus yield results for the QCD thermodynamics which agree very well with lattice QCD for all temperatures  $T \gtrsim 2.5T_c$  [7]. Underlying such resummation schemes, there is the picture of QGP as a gas of weakly interacting ‘quasiparticles’ — quarks and gluons with energies and momenta of order  $T$  which are ‘dressed’ by medium effects.

But this picture, which would be natural at weak coupling, has been shaken by some of the experimental discoveries at RHIC [8], especially the unexpectedly large ‘elliptic flow’ and ‘jet quenching’, which are rather suggestive of strong coupling [6, 9].

The ‘elliptic flow’ refers to an azimuthal anisotropy in the distribution of the particles produced in a peripheral nucleus–nucleus collision. Such a pattern is natural for a *fluid*, which is a system with strong interactions, but it would be very difficult to explain for a weakly coupled gas. The elliptic flow measured at RHIC [8] not only is strong, but it is so even for the heavy quarks  $c$  and  $b$ , which appear to be dragged by the medium in spite of their large masses. The RHIC data for elliptic flow can be well accommodated within theoretical analyses using hydrodynamics, which assume early thermalization ( $\tau_0 \lesssim 1$  fm/c) and small viscosity — more precisely, a very small viscosity to entropy–density ratio  $\eta/s$ . These features are signatures of a system with strong interactions: indeed, when  $g \ll 1$ , both the equilibration time  $\tau_0$  and the ratio  $\eta/s$  are parametrically large, since proportional to the mean free path  $\sim 1/g^4$ . On the other hand, AdS/CFT calculations for gauge theories with a gravity dual [10] suggest that, in the limit of an infinitely strong coupling, the ratio  $\eta/s$  should approach a universal lower bound which is  $\hbar/4\pi$  [11]. Interestingly, it appears that, within the error bars, the ratio  $\eta/s$  extracted (via the theoretical analyses) from the RHIC data [12] is rather close to this lower bound, thus supporting the new paradigm of a *strongly coupled Quark–Gluon Plasma* (sQGP).

Whereas the elliptic flow is a manifestation of long–range correlations which could be indeed sensitive to larger values of the coupling, the observation of strong–coupling aspects in relation with ‘jet quenching’ looks even more surprising, since it seems to be in conflict with asymptotic freedom. The ‘jet quenching’ refers to the energy loss and transverse momentum broadening of an energetic parton (the ‘jet’) which interacts with the medium. The jet has a relatively large transverse momentum  $k_\perp \gg T$  and hence it explores the structure of the plasma on relatively small space–time distances  $\ll 1/T$  (‘hard probe’). Some typical values at RHIC are  $k_\perp \sim 2 \div 20$  GeV and  $T \sim 0.5$  GeV. Because of this large separation in scales, one would expect the medium to be relatively transparent for the jets, but the measurements at RHIC show that this is actually not the case: the

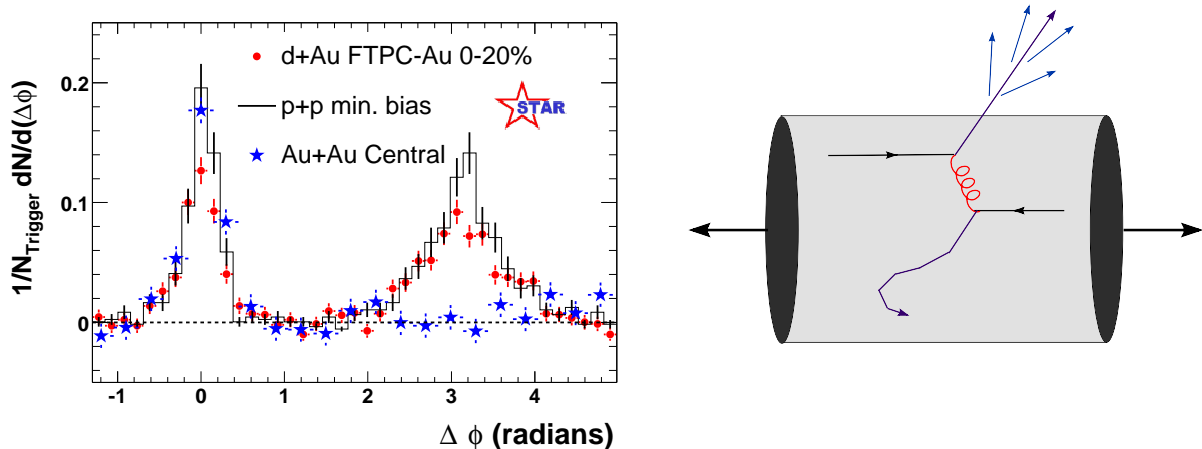


Figure 1: *Left: Azimuthal correlations for jet measurements ( $k_{\perp}(assoc) > 2$  GeV) at RHIC (STAR) in p+p, d+Au, and Au+Au collisions. Right: Jet production in a nucleus–nucleus collision.*

medium appears to be opaque [8].

This opaqueness is manifest e.g. in the RHIC measurements of the ‘nuclear modification factor’ — the ratio  $R_{AA}$  between the particle yield in Au+Au collisions and the respective yield in proton–proton collisions scaled up by  $A^2$ . This ratio would be one in the absence of medium effects, but in reality one finds a much lower value,  $R_{AA} \simeq 0.2 \div 0.3$ , which is interpreted as a sign of strong energy loss in the medium. Another observable which points in the same direction is the ‘away–jet suppression’ observed in the azimuthal correlations of the produced jets: unlike in p+p or d+Au collisions, where the hard particles typically emerge from the collision region as pairs of back–to–back jets, in the Au+Au collisions at RHIC one sees ‘mono–jet’ events in which the second jet is missing (see Fig. 1 left). This has the following natural interpretation (see Fig. 1 right): the hard scattering producing the jets has occurred near the edge of the interaction region, so that one of the jets has escaped and triggered a detector, while the other one has been deflected, or absorbed, via interactions in the surrounding medium.

Assuming weak coupling, it is possible to compute energy loss and momentum broadening within perturbative QCD [13]. If the medium is composed of weakly interacting quasiparticles (quarks and gluons), then the deflection of the hard jet is due to its successive scattering off these quasiparticles (see Fig. 2 left). Also, energy loss at weak coupling is dominated by *medium induced radiation*, that is, the emission of a hard gluon in the presence of medium rescattering. Both phenomena are controlled by the same transport coefficient, the ‘jet quenching parameter’  $\hat{q}$ , defined as the rate of transverse momentum broadening. In pQCD  $\hat{q}$  is estimated as the cross–section for the scattering between the jet and the plasma constituents ‘seen’ by the jet on its hard resolution scale. At high energy, these constituents are mostly gluons and  $\hat{q}$  is estimated as [13]

$$\hat{q} \equiv \frac{d\langle k_{\perp}^2 \rangle}{dt} \simeq \frac{\alpha_s N_c}{N_c^2 - 1} \mathcal{G}(x, Q^2), \quad (1)$$

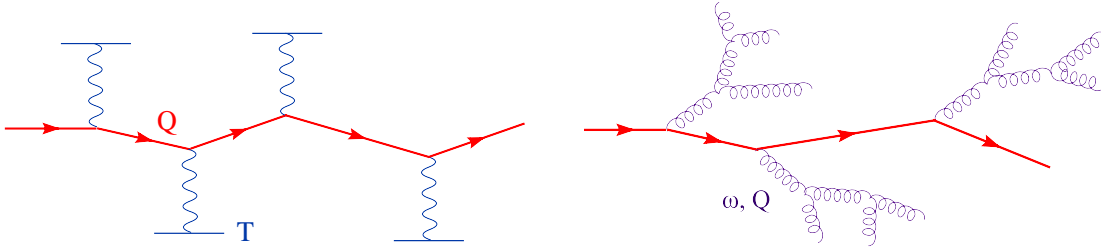


Figure 2: *Transverse momentum broadening for a heavy quark which propagates through a quark–gluon plasma. Left: weak coupling (successive scattering off thermal quasiparticles). Right: strong coupling (medium induced branching).*

where  $\mathcal{G}(x, Q^2)$  is the gluon distribution in the medium on the resolution scale  $Q^2 \sim \langle k_\perp^2 \rangle$ , as produced via the quantum evolution of the quasiparticles from their intrinsic energy scale to the hard scale  $Q$  (see Fig. 3). For instance, if the medium is a finite-temperature plasma with temperature  $T$ , then  $\mathcal{G} \simeq n_q(T) \mathcal{G}_q + n_g(T) \mathcal{G}_g$ , where  $n_{q,g}(T) \propto T^3$  are the quark and gluon densities in thermal equilibrium and  $\mathcal{G}_{q,g}(x, Q^2)$  are the gluon distributions produced by a single quark, respectively gluon, on the scale  $Q \gg T$ .  $\hat{q}$  is also related to the saturation scale  $Q_s$  in the plasma, via  $Q_s^2 \simeq \hat{q}L$  where  $L$  is the longitudinal extent of the medium. At weak coupling, one can evaluate all these quantities within pQCD. By doing that, one finds an estimate  $\hat{q}_{\text{pQCD}} \simeq (0.5 \div 1) \text{GeV}^2/\text{fm}$ , while phenomenology [14, 15] rather suggests that  $\hat{q}$  should be somehow larger, between 5 and 15  $\text{GeV}^2/\text{fm}$ . One should nevertheless keep in mind that this phenomenology is quite difficult and not devoid of ambiguities: strong assumptions are necessary in order to compute  $\hat{q}$ , and also to extract its value from the RHIC data (see, e.g., the discussion in [16]).

This discrepancy suggests that the actual gluon distribution in the plasma is significantly larger than expected in pQCD. A possible explanation for that is a stronger value for the coupling, which would enhance the quantum evolution from  $T$  up to  $Q$ . Note that there is not necessarily a conflict with asymptotic freedom: to get an enhanced gluon distribution on the relatively hard scale  $Q$ , it is enough to have a stronger coupling at the lower end of the evolution, that is, at the relatively soft scale  $T$  (where we know that  $g \simeq 2$  is indeed quite large). Actually, in Ref. [17] we proposed a strategy for numerically studying this evolution in lattice QCD at finite temperature and thus directly test the hypothesis of strong coupling.

### 3. The AdS/CFT correspondence

The previous discussion invites us to a better understanding of parton evolution and saturation in deconfined QCD matter at strong coupling, that is, for  $\alpha_s \equiv g^2/4\pi \simeq 1$ . However, even without the complications of confinement, the QCD calculations at strong coupling remain notoriously difficult. (In particular, lattice QCD cannot be used for real-time phenomena so like scattering.) So it has become common practice to look to the  $\mathcal{N} = 4$  supersymmetric Yang–Mills (SYM) theory, whose strong coupling regime can be addressed within the AdS/CFT correspondence, for guidance as to general properties of

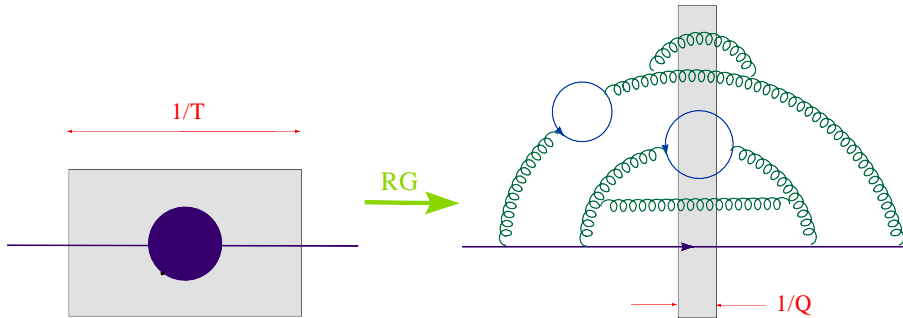


Figure 3: Parton evolution from the thermal scale  $T$  up to the harder scale  $Q \gg T$ .

strongly coupled plasmas (see the review papers [18, 19, 20]).

$\mathcal{N} = 4$  SYM has the ‘color’ gauge symmetry  $SU(N_c)$ , so like QCD, but differs from the latter in some other aspects: it has conformal symmetry (the coupling  $g$  is fixed) and no confinement, and all the fields in its Lagrangian (gluons, scalars, and fermions) transform in the adjoint representation of  $SU(N_c)$ . But these differences are believed not to be essential for a study of the quark–gluon plasma phase of QCD in the temperature range of interest for heavy ion collisions at RHIC and LHC ( $2T_c \lesssim T \lesssim 5T_c$ ), where QCD itself is known (e.g., from lattice studies [21]) to be nearly conformal.

The AdS/CFT correspondence [22, 23, 24] is the statement that the conformal field theory (CFT)  $\mathcal{N} = 4$  SYM is ‘dual’ (*i.e.*, equivalent) to a specific string theory (‘type IIB’) living in a  $(9 + 1)$ –dimensional space time with  $AdS_5 \times S^5$  geometry. The 5–dimensional Anti-de-Sitter space–time  $AdS_5$  is a space with Lorentz signature and uniform negative curvature and can be roughly imagined as the direct product between our  $(3 + 1)$ –dimensional Minkowski world and a radial, or ‘fifth’, dimension  $\chi$ , with  $0 \leq \chi < \infty$ . Our physical world is the boundary of  $AdS_5$  at  $\chi = 0$  (see the sketch in Fig. 4). The radial dimension is, roughly speaking, dual to the virtual momenta of the quantum fluctuations that we implicitly integrate out in the boundary gauge theory (see the discussion in Sect. 4).

This gauge/string equivalence is conjectured to hold for arbitrary values of the parameters  $g$  and  $N_c$ , but in practice this is mostly useful in the strong ‘t Hooft coupling limit  $\lambda \equiv g^2 N_c \rightarrow \infty$  with  $g \ll 1$ , where the string theory becomes tractable — it reduces to classical gravity in 9+1 dimensions (‘supergravity’). This limit is generally not a good limit for studying scattering, since the respective amplitudes are suppressed as  $1/N_c^2$  [25, 26]. Yet, this is meaningful for processes taking place in a deconfined plasma, which involves  $N_c^2$  degrees of freedom per unit volume, thus yielding finite amplitudes when  $N_c \rightarrow \infty$ . The gravity dual of the  $\mathcal{N} = 4$  SYM plasma with temperature  $T$  is obtained [27] by introducing a black–hole (BH) in the radial dimension of  $AdS_5$  — something that may look natural, given that a BH has entropy and thermal (Hawking) radiation. The BH horizon is located at  $\chi = 1/T$  and is parallel to the Minkowski boundary — that is, the BH is homogeneous in the physical 4 dimensions. One can see here a manifestation of the *ultraviolet/infrared correspondence* (or ‘holographic principle’), which is very useful for the physical interpretation of the supergravity calculations: the presence of a gravitational source at a distance  $\chi_0$  in the bulk of  $AdS_5$  (here the BH horizon at  $\chi_0 = 1/T$ ) corresponds

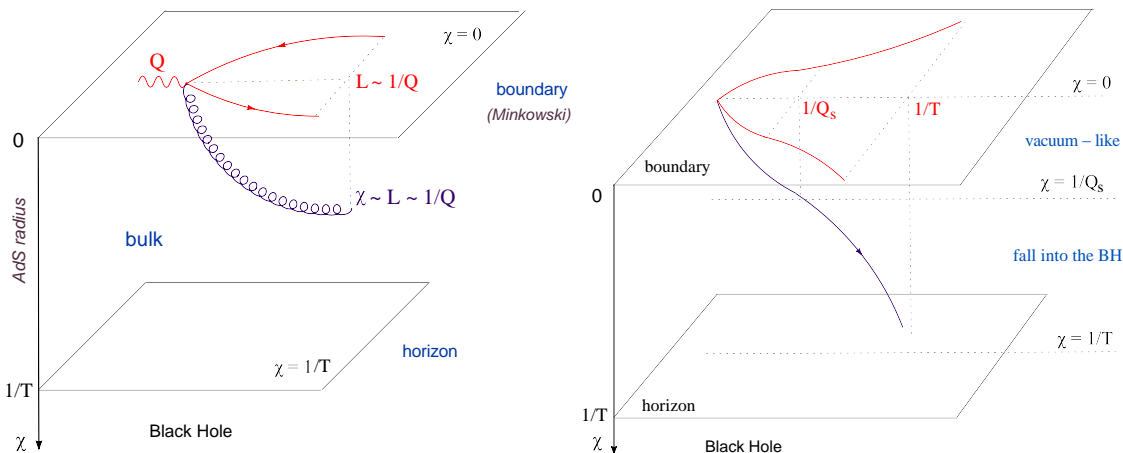


Figure 4: *Space-like current in the plasma: the trajectory of the wave packet in  $AdS_5$  and its ‘shadow’ on the boundary. Left: low energy — the Maxwell wave gets stuck near the boundary. Right: high energy — the wave falls into the BH.*

to adding a energy/momentum scale  $1/\chi_0$  in the boundary gauge theory (here, the plasma with temperature  $T$ ).

#### 4. Deep inelastic scattering at strong coupling

To understand parton evolution at strong coupling, we need a non-perturbative and gauge-invariant definition of the concept of ‘parton’, which can be extrapolated to AdS/CFT. This is provided by deep inelastic scattering (DIS), which in its essence describes the absorption of a space-like photon by the constituents of the target hadron which carry electric charge. The respective cross-section — the ‘structure function’  $F_2(x, Q^2)$  — is a direct measure of the distribution of these charged partons (the quarks in the case of QCD) on the resolution scales  $x$  and  $Q^2$  of the virtual photon. Here  $Q^2$  is the photon virtuality and fixes the typical transverse momentum (or inverse transverse size) of the struck quark. Furthermore  $x \equiv Q^2/(2q \cdot P) \approx Q^2/s$ , with  $s$  the invariant energy squared of the proton-photon system, is the Bjorken- $x$  variable and fixes the longitudinal resolution of the photon: the struck quark carry a fraction  $x$  of the hadron longitudinal momentum  $P$ . At weak coupling at least, the gluon distribution can be extracted too from the measured  $F_2(x, Q^2)$ , by using the perturbative evolution equations for the parton distributions.

Using the AdS/CFT correspondence we have computed DIS off the  $\mathcal{N} = 4$  SYM plasma at temperature  $T$  and in the strong coupling (or large- $N_c$ ) limit [28, 29]. The virtual photon couples to the constituents of the plasma which carry the  $\mathcal{R}$ -charge (the analog of the electromagnetic charge in  $\mathcal{N} = 4$  SYM). The dual, supergravity, picture of DIS is as follows (see Fig. 4) : the  $\mathcal{R}$ -current  $J_\mu$  acts as a perturbation on the Minkowski boundary of  $AdS_5$  at  $\chi = 0$ , thus inducing a massless, vector, supergravity field  $A_m$  (with  $m = \mu$  or  $\chi$ ) which propagates towards the bulk of  $AdS_5$  ( $\chi > 0$ ), according to Maxwell

equations in curved space–time<sup>1</sup> :

$$\partial_m(\sqrt{-g}g^{mp}g^{nq}F_{pq}) = 0, \quad \text{where } F_{mn} = \partial_m A_n - \partial_n A_m. \quad (2)$$

These equations describe the gravitational interaction between the Maxwell field  $A_m$  and the BH (implicit in the 5–dimensional metric tensor  $g^{mn}$ ). Note that there is no explicit coupling constant in the equations: the gravitational scattering is rather controlled by the kinematics. Given the solution  $A_m$ , there is a well–identified procedure to construct the current–current correlator  $\langle J_\mu(x)J_\nu(y) \rangle$  in the boundary gauge theory. Then, the DIS structure function is finally obtained by taking the imaginary part of this correlator in momentum space, like usual.

Eqs. (2) remain non–trivial even at  $T = 0$ , in which case they describe the propagation of the virtual photon through the vacuum of the strongly–coupled  $\mathcal{N} = 4$  SYM theory. The physical interpretation of the results can be deduced using the UV/IR correspondence alluded to above, which is more precisely formulated as follows [28, 29]: the radial penetration  $\chi$  of the Maxwell field  $A_m$  in  $AdS_5$  is proportional to the transverse size  $L$  of the typical quantum fluctuations of the virtual photon in the boundary gauge theory.

As an example, consider the  $T = 0$  case: as well known, a space–like photon cannot decay into on–shell (massless) quanta in the vacuum, because of energy–momentum conservation. Rather it fluctuates into a virtual system of partons, whose complexity can be very high at strong coupling, but whose space–time delocalization is fixed by the uncertainty principle: in a frame where the photon has 4–momentum  $q^\mu = (\omega, 0, 0, q)$  and (space–like) virtuality  $Q^2 = q^2 - \omega^2 > 0$ , its virtual fluctuations have a typical transverse size  $L \sim 1/Q$  and a longitudinal size, or lifetime,  $\Delta t \sim \omega/Q^2$ . And indeed, the solutions to Eqs. (2) at  $T = 0$  show that the wave–packet representing  $A_m$  penetrates into the bulk up to a maximal distance  $\chi \sim 1/Q$  and the propagation time from the boundary up to that maximal distance is  $\sim \omega/Q^2$  [29]. The requirement of energy–momentum conservation enters the AdS calculation in the form of a repulsive barrier around  $\chi \sim 1/Q$  which prevents the wave packet to penetrate further down into  $AdS_5$ .

The same repulsive barrier, with a height  $\propto Q^2$ , shows up also at finite temperature<sup>2</sup>, but in that case there is also an attractive interaction  $\propto \omega^2 T^4$ , namely the gravitational attraction by the BH. The physical interpretation of the latter in the dual gauge theory is quite subtle [28] and will emerge from the arguments below. The competition between these two interactions depends upon the kinematics. For sufficiently low energy  $\omega$ , such that  $\omega T^2 \ll Q^3$ , the repulsive barrier wins and then the Maxwell field is stuck within a distance  $\chi \lesssim 1/Q \ll 1/T$  from the Minkowski boundary, so like in the vacuum (cf. Fig. 4 left). In this regime there is essentially no interaction with the black hole, meaning no absorption of the virtual photon by the plasma, and hence no DIS. But for higher energies and/or temperatures, such that  $\omega T^2 \gtrsim Q^3$ , the attraction wins and then the wave–packet falls into the BH horizon, from which it cannot escape back anymore (cf. Fig. 4 right): the space–like photon is completely absorbed into the plasma.

---

<sup>1</sup>The 5–dimensional sphere ( $S^5$ ) part of  $AdS_5 \times S^5$  plays no role for this particular calculation.

<sup>2</sup>The photon has 4–momentum  $q^\mu = (\omega, 0, 0, q)$  in the plasma rest frame and we assume that  $Q^2 \equiv q^2 - \omega^2 \gg T^2$ , as appropriate for hard probes.



To understand the existence of these two regimes, it is useful to note that the ‘criticality’ condition for having strong interactions, that is  $\omega T^2 \sim Q^3$ , can be rewritten as

$$Q \sim \frac{\omega}{Q^2} T^2, \quad (3)$$

with the following interpretation [28] : the scattering becomes strong when the lifetime  $\Delta t \sim \omega/Q^2$  of the partonic fluctuation is large enough for the mechanical work  $W = \Delta t \times F_T$  done by the *plasma force*  $F_T \sim T^2$  acting on these partons to compensate for their energy deficit  $\sim Q$ . This mechanical work allows the partons to become (nearly) on-shell — or more precisely to reduce their virtuality from the original value  $Q \gg T$  down to a value of order  $T$ . When this happens, the fluctuation *thermalizes* — the partons become a part of the thermal bath — and the photon disappears into the plasma.

This plasma force  $F_T \sim T^2$  represents (in some average way) the effect of the strongly-coupled plasma on partonic fluctuations and can be viewed as a prediction of the AdS/CFT calculation. Note that one cannot interpret this force in terms of individual collisions between the virtual photon and some ‘plasma constituents’ : the BH dual to the plasma is homogeneous in the four physical dimensions, hence it cannot transfer any 4-momentum to the photon, so like a genuine scattering would do (recall, e.g., Fig. 2 left). Rather, this is a kind of *tidal force* which pulls the partons apart until they disappear in the plasma. The emergence of a tidal force, which is a hallmark of gravitational interactions, in the context of a gauge theory may look surprising, but in fact this is not more mysterious than the basic paradigm of the gauge/gravity duality — the fact that a gauge theory at strong coupling can be effectively described as gravity. Further insight in that sense comes from an argument [25] based on the operator product expansion (OPE): among the infinitely many leading-twist operators which *a priori* contribute to OPE for DIS, there is only one which survives in the strong coupling limit — the energy-momentum tensor  $T_{\mu\nu}$ . All the other operators acquire large, negative, anomalous dimensions  $\propto \lambda^{1/4}$  and thus are strongly suppressed when  $\lambda \rightarrow \infty$ . (See also the discussion in Sect. 5.) Accordingly, one expects the theory of scattering in a gauge theory at strong coupling to be an effective theory for  $T_{\mu\nu}$ . By covariance, this must be a gravity theory.

## 5. Parton saturation at strong coupling

The OPE argument alluded to above also helps clarifying the *partonic picture* of the AdS/CFT results for DIS at strong coupling [28, 29], to which I now turn. To formulate this picture, one needs to use the DIS variables  $Q^2 = q^2 - \omega^2$  and  $x = Q^2/(2\omega T)$ . As previously mentioned, the AdS calculation allows one to deduce the DIS structure function  $F_2(x, Q^2)$  from the imaginary part of the current-current correlator. The discussion in the previous section suggests that there should be a dramatic change in  $F_2(x, Q^2)$  at the critical kinematics defined by the condition in Eq. (3). The latter can be rewritten as  $Q_s(\omega) \simeq (\omega T^2)^{1/3}$  or, in terms of the DIS variables,

$$Q_s(x) \simeq \frac{T}{x}, \quad \text{or} \quad x_s(Q) \simeq \frac{T}{Q}. \quad (4)$$

Any of these equations defines a line in the kinematical plane  $(x, Q^2)$ , which for reasons to shortly become clear is dubbed the *saturation line*. The AdS results for DIS off the strongly coupled plasma can then be summarized as follows [28] :

(i) For relatively low energy, or high  $Q^2$ , such that  $x > x_s(Q)$ , the scattering is negligible and  $F_2(x, Q^2) \approx 0$ . (More precisely, there is a small contribution to  $F_2$  produced via tunneling across the repulsive barrier, but this is exponentially suppressed.)

(ii) For higher energies, or lower  $Q^2$ , such that  $x \lesssim x_s(Q)$ , the scattering is strong and the structure function is non-zero and parametrically large:  $F_2(x, Q^2) \sim x N_c^2 Q^2$ .

These results are consistent with the energy-momentum sum-rule, which requires the integral  $\int_0^1 dx F_2(x, Q^2)$  to have a finite limit as  $Q^2 \rightarrow \infty$ . (This is simply the statement that the total energy per unit length in the plasma is the same whatever is the resolution scale  $Q^2$  on which one measures this energy: by varying  $Q^2$  one merely changes the nature and size of the partons which carry that energy, cf. Fig. 3, but their cumulated energy remains the same.) Using the above results, one finds indeed

$$\int_0^1 dx F_2(x, Q^2) \simeq \int_0^{x_s} dx F_2(x, Q^2) \simeq x_s F_2(x_s, Q^2) \sim N_c^2 T^2, \quad (5)$$

where the integral is dominated by values  $x \simeq x_s(Q)$ .

The physical interpretation of these results becomes transparent after recalling that the variable  $x$  represents the longitudinal momentum fraction of the plasma constituent which absorbs the virtual photon. Then the above statement (i) implies that there are no partons at large  $x$ , or high  $Q^2$ : the strongly coupled plasma has no point-like constituents. Also, statement (ii) together with Eq. (5) show that the total energy of the plasma as measured on a hard resolution scale  $Q^2 \gg T^2$  is carried by very soft constituents with small values of  $x \simeq x_s(Q) \ll 1$ .

This picture at strong coupling is very different from that of an energetic hadron in QCD, as predicted by perturbative QCD and confirmed by many experimental data [3]. In that case, the hadronic wavefunction at high energy is dominated by small- $x$  partons (mostly gluons), as produced via bremsstrahlung from partons with larger  $x$ . Yet, the hadron energy is concentrated in the few partons with larger values of  $x$  (the ‘valence partons’); that is, the energy-momentum sum rule is saturated by  $x \sim 0.3$ . Moreover these valence partons are seen on all scales of  $Q^2$ , that is, there are *point-like*.

This rises the following questions: why and how did partons disappear at strong coupling? And what is the nature of the small- $x$  constituents which carry the plasma energy on the hard resolution scale  $Q^2$ ? A first hint in that sense comes again from the OPE for DIS [25]. The twist-two operators which enters OPE probe the distribution of energy among the partons inside the hadron: the hadron expectation value of the spin- $n$  twist-2 operator  $\mathcal{O}^{(n)}$  is proportional to the  $(n-1)$ -th moment of the longitudinal momentum fraction  $x$  carried by the quark and gluon constituents of that hadron:

$$\langle x^{n-1} \rangle_{Q^2} \equiv \int_0^1 dx x^{n-2} F_2(x, Q^2) \propto \langle \mathcal{O}^{(n)} \rangle_{Q^2}. \quad (6)$$

As indicated in this equation, the operators depend upon the resolution scale  $Q^2$ , because of the quantum evolution illustrated in Fig. 3. In a conformal theory at strong cou-

pling, all such operators except for  $T_{\mu\nu}$  are strongly suppressed at large  $Q^2$ :  $\mathcal{O}^{(n)}(Q^2) \propto (T^2/Q^2)^{\lambda^{1/4}} \rightarrow 0$ . Via Eq. (6) this implies  $\langle x^{n-1} \rangle_{Q^2} \rightarrow 0$  for any  $n > 2$ , which suggest a very rapid evolution towards  $x = 0$ . This is in fact natural at strong coupling, where one expects a *very efficient parton branching*. Unlike at weak coupling, where parton radiation is suppressed by powers of the coupling and thus favors the emission of soft (small  $x$ ) and collinear (small  $k_\perp$ ) gluons — for which the bremsstrahlung probability is kinematically large —, at strong coupling there is no such a suppression anymore, and phase-space considerations alone favor a ‘quasi-democratic’ branching [28, 29]: the energy and momentum of the parent parton are almost equally divided among the daughter partons. (Soft and collinear emissions play no special role at strong coupling, since they happen very slowly.) Via successive branchings, all the parton will rapidly fall to small values of  $x$  — actually the smallest one which are still consistent with energy–momentum conservation (in the sense of the sum rule (5)). That is, at strong coupling partons should still exist, but their distributions should be concentrated at very small values of  $x$ . This picture is indeed consistent with our previous findings for the strongly coupled plasma.

One may furthermore wonder what is the mechanism which is responsible for stopping the parton branching at sufficiently small values of  $x$  and which determines the specific  $Q$ –dependence of the critical value  $x_s(Q)$  — or, vice-versa, the specific  $x$ –dependence of the ‘saturation momentum’  $Q_s(x)$ . In Ref. [28] we have proposed that this mechanism is *parton saturation*: the partons keep branching until their phase-space occupation numbers — the number of partons of a given color per unit transverse phase space ( $b_\perp, k_\perp$ ) and unit rapidity  $Y \equiv \ln(1/x)$  — become of  $\mathcal{O}(1)$ :

$$\frac{1}{N_c^2} \frac{dN}{dY d^2b_\perp d^2k_\perp} \simeq 1 \quad \text{for} \quad k_\perp \lesssim Q_s(x) = \frac{T}{x}. \quad (7)$$

This interpretation follows from the AdS/CFT result for the  $F_2(x, Q^2)$  at  $Q \lesssim Q_s(x)$ , as shown before, together with the observation that the quantity  $(1/x)F_2(x, Q^2)$  is essentially the number of partons in the plasma per unit area per unit rapidity as ‘seen’ by a virtual photon with resolution  $Q$ :

$$\frac{1}{x} F_2(x, Q^2) \simeq \int^Q d^2k_\perp \frac{dN}{dY d^2b_\perp d^2k_\perp} \sim N_c^2 Q^2 \quad \text{for} \quad Q \lesssim Q_s(x). \quad (8)$$

This interpretation is appealing in that it suggests some continuity in the physics of saturation and unitarization from weak to strong coupling: saturation occurs when the occupation numbers are high enough for the repulsive interactions among the partons to prevent further radiation [3]. At weak coupling, this requires large gluon occupation numbers, of order  $1/\alpha_s$ , in order to compensate for the weakness of the repulsive interactions. But at strong coupling, one can think of the individual partons as ‘hard disks’ with transverse area  $1/k_\perp^2$ ; then saturation occurs when these disks start to touch with each other, *i.e.* for occupation numbers of order one.

But, clearly, there are important differences between the parton picture at weak and respectively strong coupling. These differences are most striking outside the saturation region, at  $k_\perp \gg Q_s(x)$ , where at strong coupling there are no partons at all, whereas

at weak coupling the parton distributions show large ‘leading–twist’ tails, which in fact dominate the phenomenology at both HERA and LHC. Another important difference refers to the energy dependence of the saturation momentum  $Q_s$ . At weak coupling, this is determined by the rate for gluon emission via bremsstrahlung, and more precisely by the BFKL evolution. This predicts  $Q_s^2 \sim 1/x^\omega$  where the ‘BFKL intercept’  $\omega$  is parametrically of  $\mathcal{O}(\alpha_s N_c)$  and numerically  $\omega \simeq 0.2 \div 0.3$  — in agreement with the HERA data [3]. At strong coupling we have found a much faster increase with  $1/x$ , namely  $Q_s^2(x) \propto 1/x^2$ , but one factor  $1/x$  out of this result is simply a kinematical effect, related to our study of an *infinite* plasma. That is, one should understand the above result as  $Q_s^2(x) \propto \Delta t/x$ , where  $\Delta t \sim \omega/Q^2 \sim 1/xT$  is the lifetime of the partonic fluctuation: since the medium is infinite, the effects of the interactions accumulate all the way along the parton lifetime. As for the other factor  $1/x$ , this exhibits the ‘graviton intercept’  $j - 1 = 1$  ( $j = 2$  is the spin of the graviton) and reflects the fact that the interactions responsible for DIS at strong coupling involve exchanges of the energy–momentum tensor — the only operator which survives in OPE at strong coupling.

The above discussion also suggests how our result for  $Q_s^2(x)$  should change when, instead of an infinite plasma, we consider a slice of the plasma with longitudinal size  $L_z \ll \omega/Q^2$ . In that case one expects

$$Q_s^2(x, T, L_z) \sim \frac{T^3 L_z}{x} \quad (\text{slice of the plasma with } L_z \ll 1/xT), \quad (9)$$

and this is indeed confirmed by the respective AdS/CFT calculation [30, 31]. Such a ‘slice of the plasma’ may be viewed as a rough model for a ‘nucleus’ in  $\mathcal{N} = 4$  SYM (which however involves  $N_c^2$  degrees of freedom per unit volume) [32, 33, 34, 35].

## 6. High–energy scattering at strong coupling

The previously described parton picture implies that high–energy processes taking place in the *vacuum* of an hypothetical world which is conformal and strongly coupled would look quite different from the corresponding processes in QCD. For instance, the absence of large– $x$  partons means that, in the collision between two strongly coupled hadrons, there is no particle production at forward and backward rapidities. This is in sharp contrast to the situation at RHIC, where the large– $x$  partons from the incoming nuclei are seen to emerge from the collision, as hadronic jets, along their original trajectories.

A related prediction of AdS/CFT is the absence of jets in electron–positron annihilation at strong coupling [28, 36]. Fig. 5 exhibits the typical, 2–jet, final state in  $e^+e^-$  annihilation at weak coupling (left) together with what should be the corresponding state at strong coupling (right). In both cases, the final state is produced via the decay of a time–like photon into a pair of partons and the subsequent evolution of this pair. At weak coupling this evolution typically involves the emission of soft and collinear gluons, with the result that the leading partons get dressed into a pair of well–collimated jets of hadrons (cf. Fig. 5 left). At strong coupling, parton branching is much more efficient, as previously explained, and rapidly leads to a system of numerous and relatively soft quanta,

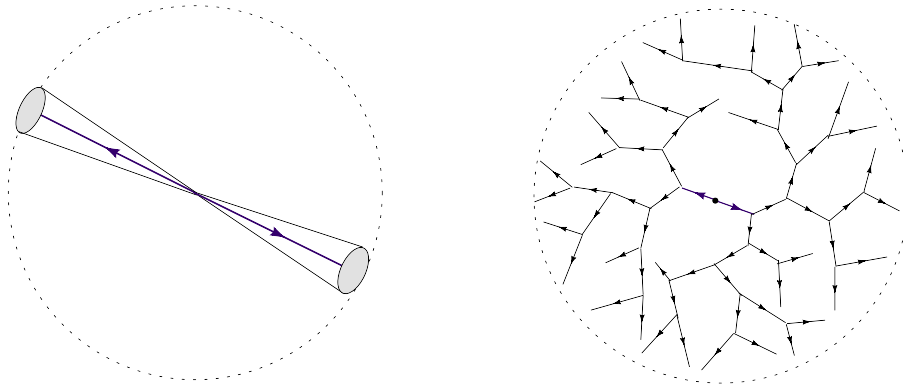


Figure 5:  $e^+e^-$  annihilation. Left: weak coupling. Right: strong coupling.

with energies and momenta of the order of the confinement scale, which are isotropically distributed in space (cf. Fig. 5 right) [36].

But such discrepancies should not come as a surprise: after all, we know that hard processes in high energy QCD are governed by weak coupling and perturbative QCD does a good deal in predicting the respective cross-sections. As for the softer processes in the vacuum, so like hadronization, for which  $\alpha_s \sim 1$ , these are largely controlled by confinement and hence they remain out of the reach of the AdS/CFT techniques. Remember however that our original motivation for studying high-energy processes at strong coupling is rather related to the *quark-gluon plasma*, where there is no confinement and the coupling might indeed be quite strong.

So let me finally return to this topic and consider the propagation of a ‘hard probe’ — say, a heavy quark — through a strongly-coupled plasma. The string theory dual of a heavy quark is a Nambu-Goto string hanging down from the boundary of AdS<sub>5</sub> and propagating through the AdS<sub>5</sub> black hole space-time. By solving the corresponding equations of motion, it has been possible to compute both the quark energy loss [37, 38] and its momentum broadening [39, 40, 41] at strong coupling. The physical interpretation of the results [34, 41] turns out to be quite interesting: unlike in perturbative QCD, the dominant mechanism at work is not thermal rescattering (cf. Fig. 2 left), but rather *medium-induced parton branching* (cf. Fig. 2 right).

The corresponding physical picture is in fact quite similar to that of DIS, as discussed in Sect. 4. The heavy quark can emit space-like quanta of  $\mathcal{N} = 4$  SYM, which in the vacuum would have only a finite lifetime  $\Delta t \simeq \omega/Q^2$ ; after that time, they would be reabsorbed by the heavy quark. (As usual,  $\omega$  and  $Q$  refers to the energy and the virtuality of the emitted quanta.) However, in the presence of the plasma, those quanta having a virtuality  $Q$  lower than  $Q_s(\omega)$  can escape into the medium, and thus provide energy loss and momentum broadening. Here,  $Q_s(\omega) \simeq (\omega T^2)^{1/3}$  is the plasma saturation momentum on the energy scale of the fluctuation, cf. Eq. (3).

Based on this physical picture, it is possible to estimate the rate for energy loss: each emission brings in an energy loss  $\Delta E \simeq \omega$  over a time  $\Delta t$ , so the corresponding rate  $dE/dt$  is proportional to  $\omega/\Delta t \simeq Q^2 \lesssim Q_s^2(\omega)$ . Hence, the energy loss is dominated by

those fluctuations having the maximal possible energy  $\omega_{\max}$  and a virtuality equal to the corresponding saturation momentum:  $Q \simeq Q_s(\omega_{\max})$ . More precisely, the quantity which is limited is not the energy  $\omega$  of a quanta, but its ‘rapidity’  $\gamma_p \equiv \omega/Q$  (the Lorentz boost factor): this cannot exceed the rapidity  $\gamma = 1/\sqrt{1-v^2}$  of the heavy quark (which is here assumed to propagate at constant speed  $v$ ). It is therefore appropriate to reexpress  $Q_s$  as a function of  $\gamma_p$ , by successively writing  $Q_s \simeq (\omega T^2)^{1/3} = (\gamma_p Q_s T^2)^{1/3} = \sqrt{\gamma_p} T$ . This quantity takes a maximal value  $(Q_s)_{\max} = \sqrt{\gamma} T$ , thus yielding the following estimate for the rate for energy loss (below,  $Q_s \equiv (Q_s)_{\max}$ ):

$$-\frac{dE}{dt} \simeq \sqrt{\lambda} \frac{\omega}{(\omega/Q_s^2)} \simeq \sqrt{\lambda} Q_s^2 \sim \sqrt{\lambda} \gamma T^2. \quad (10)$$

The additional factor  $\sqrt{\lambda}$  comes from the fact that, at strong coupling, the heavy quark does not radiate just a single quanta per time  $\Delta t$ , but rather a large number  $\sim \sqrt{\lambda}$ . Eq. (10) is parametrically consistent with the respective AdS/CFT result [37, 38].

One can similarly estimate the momentum broadening: the  $\sqrt{\lambda}$  quanta emitted during  $\Delta t$  are uncorrelated with each other, so they randomly modify the transverse momentum of the heavy quark, by a typical amount  $\Delta k_{\perp} \sim Q_s$  per emission. Such random changes add in quadrature, thus yielding

$$\frac{d\langle k_{\perp}^2 \rangle}{dt} \sim \frac{\sqrt{\lambda} Q_s^2}{(\omega/Q_s^2)} \sim \sqrt{\lambda} \frac{Q_s^4}{\gamma Q_s} \sim \sqrt{\lambda} \sqrt{\gamma} T^3, \quad (11)$$

in agreement with the explicit calculations in Refs. [39, 40, 41]. Note the strong enhancement of the medium effects at high energy, as expressed by the Lorentz  $\gamma$  factor in Eqs. (10) and (11): this might qualitatively explain the strong suppression of particle production seen in Au+Au collisions at RHIC (cf. Sect. 2).

## 7. Conclusions

The AdS/CFT calculations summarized here demonstrate that, at least in a conformal world, parton saturation is a universal phenomenon, appearing at both weak and strong coupling, and presumably for any intermediate value of the coupling. More generally, the concept of ‘parton’ in relation with high energy scattering appears to be relevant at strong coupling as well. There are significant differences with respect to the respective picture at weak coupling, so like the absence of point-like constituents. These differences can be intuitively understood as consequences of parton evolution at strong coupling. These differences and their consequences for high-energy scattering — which look very different from the known phenomenology in QCD — rule out this conformal strong-coupling scenario as a candidate theory for high-energy processes in the vacuum. On the other hand, such methods can give us a hint towards understanding the deconfined QCD matter to be copiously produced in the intermediate stages of heavy ion collisions at LHC. In particular, they could shed light on fundamental open questions, such as the rapid thermalization, the small entropy-to-density ratio, or the strong jet quenching observed in relation with this matter at RHIC. Last but not least, by combining in a unified theoretical

framework concepts and methods coming from fields as different as gravity, string theory, quantum field theory, statistical physics, and hydrodynamics, the gauge/string duality teaches us the unity of physics.

## References

- [1] L. V. Gribov, E. M. Levin, and M. G. Ryskin, *Phys. Rept.* **100** (1983) 1.
- [2] A. H. Mueller and J.-w. Qiu, *Nucl. Phys.* **B268** (1986) 427.
- [3] E. Iancu and R. Venugopalan, “The Color Glass Condensate and High Energy Scattering in QCD” [[arXiv:hep-ph/0303204](#)];  
H. Weigert, “Evolution at small  $x_{bj}$ : The Color Glass Condensate”, *Prog. Part. Nucl. Phys.* **55** (2005) 461 [[arXiv:hep-ph/0501087](#)];  
J. Jalilian-Marian and Y. V. Kovchegov, “Saturation physics and deuteron gold collisions at RHIC”, *Prog. Part. Nucl. Phys.* **56** (2006) 104 [[hep-ph/0505052](#)];  
F. Gelis, E. Iancu, J. Jalilian-Marian, R. Venugopalan, “The Color Glass Condensate”, *Ann. Rev. Nucl. Part. Sci.* **60** (2010) 463 [[arXiv:1002.0333](#)][[hep-ph](#)].
- [4] L. D. McLerran and R. Venugopalan, *Phys. Rev.* **D49** (1994) 2233.
- [5] J. L. Albacete, N. Armesto, J. G. Milhano, and C. A. Salgado, *Phys. Rev.* **D80** (2009) 034031.
- [6] M. Gyulassy and L. McLerran, *Nucl. Phys.* **A750** (2005) 30.
- [7] J.-P. Blaizot, E. Iancu, and A. Rebhan, “Thermodynamics of the high-temperature quark gluon plasma”, [arXiv:hep-ph/0303185](#).
- [8] I. Arsene *et al.* [BRAHMS Collaboration], *Nucl. Phys.* **A757** (2005) 1;  
B. B. Back *et al.* [PHOBOS Collaboration], *Nucl. Phys.* **A757** (2005) 28;  
J. Adams *et al.* [STAR Collaboration], *Nucl. Phys.* **A757** (2005) 102 ;  
K. Adcox *et al.* [PHENIX Collaboration], *Nucl. Phys.* **A757** (2005) 184.
- [9] B. Muller, “From Quark-Gluon Plasma to the Perfect Liquid,” *Acta Phys. Polon.* **B38** (2007) 3705, [[arXiv:0710.3366](#)] [[nucl-th](#)].
- [10] G. Policastro, D. T. Son, and A. O. Starinets, *Phys. Rev. Lett.* **87** (2001) 081601.
- [11] P. Kovtun, D. T. Son, and A. O. Starinets, *Phys. Rev. Lett.* **94** (2005) 111601.
- [12] M. Luzum and P. Romatschke, *Phys. Rev.* **C78** (2008) 034915.
- [13] R. Baier, Y. L. Dokshitzer, A. H. Mueller, S. Peigne, and D. Schiff, *Nucl. Phys.* **B483** (1997) 291.
- [14] STAR Collaboration, B. I. Abelev *et al.*, *Phys. Rev. Lett.* **98** (2007) 192301.
- [15] PHENIX Collaboration, A. Adare *et al.*, *Phys. Rev. Lett.* **98** (2007) 172301.

- [16] R. Baier and D. Schiff, *JHEP* **09** (2006) 059.
- [17] E. Iancu and A. H. Mueller, *Phys. Lett.* **B681** (2009) 247.
- [18] D. T. Son and A. O. Starinets, “Viscosity, Black Holes, and Quantum Field Theory,” *Ann. Rev. Nucl. Part. Sci.* **57** (2007) 95, [arXiv:0704.0240 \[hep-th\]](#).
- [19] E. Iancu, “Partons and jets in a strongly-coupled plasma from AdS/CFT,” *Acta Phys. Polon.* **B39** (2008) 3213, [arXiv:0812.0500](#).
- [20] S. S. Gubser, S. S. Pufu, F. D. Rocha, and A. Yarom, “Energy loss in a strongly coupled thermal medium and the gauge-string duality,” [arXiv:0902.4041](#).
- [21] M. Cheng *et al.*, *Phys. Rev.* **D77** (2008) 014511.
- [22] J. M. Maldacena, *Adv. Theor. Math. Phys.* **2** (1998) 231.
- [23] S. S. Gubser, I. R. Klebanov, and A. M. Polyakov, *Phys. Lett.* **B428** (1998) 105.
- [24] E. Witten, *Adv. Theor. Math. Phys.* **2** (1998) 253.
- [25] J. Polchinski and M. J. Strassler, *JHEP* **05** (2003) 012.
- [26] Y. Hatta, E. Iancu, and A. H. Mueller, *JHEP* **01** (2008) 026.
- [27] E. Witten, *Adv. Theor. Math. Phys.* **2** (1998) 505.
- [28] Y. Hatta, E. Iancu, and A. H. Mueller, *JHEP* **01** (2008) 063.
- [29] Y. Hatta, E. Iancu, and A. H. Mueller, *JHEP* **05** (2008) 037.
- [30] A. H. Mueller, A. I. Shoshi, and B.-W. Xiao, *Nucl. Phys.* **A822** (2009) 20.
- [31] E. Avsar, E. Iancu, L. McLerran, D. N. Triantafyllopoulos, *JHEP* **11** (2009) 105.
- [32] J. L. Albacete, Y. V. Kovchegov, and A. Taliotis, *JHEP* **07** (2008) 100.
- [33] J. L. Albacete, Y. V. Kovchegov, and A. Taliotis, *JHEP* **05** (2009) 060.
- [34] F. Dominguez, C. Marquet, A. H. Mueller, B. Wu, and B.-W. Xiao, *Nucl. Phys.* **A811** (2008) 197.
- [35] S. S. Gubser, S. S. Pufu, and A. Yarom, *Phys. Rev.* **D78** (2008) 066014.
- [36] D. M. Hofman and J. Maldacena, *JHEP* **05** (2008) 012.
- [37] C. P. Herzog, A. Karch, P. Kovtun, C. Kozcaz, L. G. Yaffe, *JHEP* **07** (2006) 013.
- [38] S. S. Gubser, *Phys. Rev.* **D74** (2006) 126005.
- [39] J. Casalderrey-Solana and D. Teaney, *Phys. Rev.* **D74** (2006) 085012.
- [40] J. Casalderrey-Solana and D. Teaney, *JHEP* **04** (2007) 039.
- [41] G. C. Giecold, E. Iancu, and A. H. Mueller, *JHEP* **07** (2009) 033.